Article

Chinese Science Bulletin

Condensed Matter Physics

July 2013 Vol.58 No.20: 2413–2417
doi: 10.1007/s11434-013-5882-3

# Experimental demonstrations of high-$Q$ superconducting coplanar waveguide resonators

LI HaiJie[1], WANG YiWen[1], WEI LianFu[1,2*], ZHOU PinJia[1], WEI Qiang[1], CAO ChunHai[3], FANG YuRong[3], YU Yang[3] & WU PeiHeng[3]

[1] *Quantum Optoelectronics Laboratory, Southwest Jiaotong University, Chengdu 610031, China;*
[2] *State Key Laboratory of Optoelectronic Materials and Technologies, School of Physics and Engineering, Sun Yat-sen University, Guangzhou 510275, China;*
[3] *Research Institute of Superconductor Electronics, Nanjing University, Nanjing 210093, China*

Received November 30, 2012; accepted January 12, 2013

We successfully designed and fabricated an absorption-type of superconducting coplanar waveguide (CPW) resonators. The resonators are made from a niobium film (about 160 nm thick) on a high-resistance Si substrate, and each resonator is fabricated as a meandered quarter-wavelength transmission line (one end is short to the ground and another end is capacitively coupled to a through feedline). With a vector network analyzer we measured the transmissions of the applied microwave through the resonators at ultra-low temperature. The obtained loaded quality factors are significantly high, i.e. up to ~$10^6$. When the temperature increases slowly from the base temperature (20 mK), the resonance frequencies of the resonators are blue shifted and the quality factors are lowered slightly. In principle, this type of device can integrate a series of CPW resonators with a common feedline, making it a promising candidate as the data bus for coupling distant solid-state qubits and the sensitive detector of single photons.

**superconducting coplanar waveguide resonator, resonance frequency, quality factor**

**Citation:** Li H J, Wang Y W, Wei L F, et al. Experimental demonstrations of high-$Q$ superconducting coplanar waveguide resonators. Chin Sci Bull, 2013, 58: 2413–2417, doi: 10.1007/s11434-013-5882-3

Superconducting coplanar waveguide (CPW) resonators have been extensively studied for years, specifically as radiation detectors [1–3], parameter amplifiers [4], and the data bus of superconducting qubits [5–10]. Compared with other low temperature detectors, e.g. transition edge sensors (TESs) [11,12], superconducting tunnel junctions (STJs) [13,14], superconducting nanowire single photon detectors (SNSPDs) [15], the primary advantage of the CPW devices is that they are relatively easy to be multiplexed into large arrays. In principle, a series of CPW resonators with different frequencies can be measured using a single feedline, which greatly simplifies the system structure and relevant cryogenic electronics.

Particularly, a superconducting CPW resonator with sufficiently-high quality factor can serve as a sensitive radiation detector. Physically, the incoming photons break Cooper pairs in the superconducting resonator and create quasiparticle excitations. This changes the kinetic inductance [16] and resonance frequency of the CPW resonator, which can be easily measured experimentally. In theory, higher quality factor allows more sensitive detection of photons. Also, CPW resonators with high quality factors (i.e. with narrower 3 dB-bandwidths) imply that more resonators (with different resonant frequencies) can be multiplexed on-chip for a fixed bandwidth. This is essentially important for the development of large sensor-arrays used in astronomy [1,17–19].

Here, we report an experimental demonstration of an absorption-type of superconducting CPW resonators, which can be used as the microwave kinetic inductance detectors (MKIDs) [1,19] with high quality factors. Our device is made from a Nb film ($t$~160 nm) deposited on a high-

*Corresponding author (email: weilianfu@gmail.com)

resistance Si subtract by magnetron sputtering. The designed circuit is generated by the usual photolithography. The measured loaded quality factor of our resonator at 20 mK is $Q_l$ = 1.1654×10$^6$ at the resonant frequency $f_0$ = 1.8575 GHz. We also measured the temperature dependence of the resonance frequency in the range of base temperature (20 mK) to around 1180 mK.

## 1 Device and measurement system

The microscope photograph of our meandered CPW $\lambda/4$ transmission line resonator is shown in Figure 1. The resonator shorts to the ground plane at one end, and capacitively couples to a through line at another end. In our design, niobium is selected as the metal film material, due to its well superconductivity at low temperature. The characteristic impedance $Z_0$ of through line is designed to be 50 Ω, in order to avoid the reflections of the driving signals. In fact, for a single layer dielectric the impedance can be analytically calculated using [20]

$$Z_0 = \frac{30\pi}{\sqrt{\epsilon_{e,t}}} \frac{K(k')}{K(k)}. \quad (1)$$

Here, $\epsilon_{e,t}$ is the effective dielectric constant with a correction of the film thickness $t$, $K(k) = \int_0^{\pi/2} \mathrm{d}\theta / \sqrt{1-k^2\sin^2\theta}$ is the complete elliptic integral with modulus $k$. The parameters $k$ and $k'$ are determined by the resonator's geometry parameters [20]: the center strip width $w$, slot width between the centerstrip and the ground plane $s$, metal film thickness $t$ and the thickness $h$ of the silicon substrate. Physically, the fundamental resonance frequency $f_0$ is determined by the overall length of the CPW resonator $l$ and the effective substrate dielectric parameter $\epsilon$:

$$f_0 = \sqrt{\frac{2}{\epsilon+1}} \frac{c}{4l}. \quad (2)$$

Here, $c$ is the speed of an electromagnetic wave in a vacuum. In our design, the length of the CPW resonator is set as 15.814 mm, corresponding to a fundamental resonance frequency $f_0$ = 1.8575 GHz. Also, the center strip width $w_t$ is set as 20 μm and the slot width $s_t$ between the center strip and the ground plane is 15 μm. Note that the CPW resonator is decoupled from the through line so its impedance is not necessary to be 50 Ω.

Several aspects, e.g. coupling strength between the through line and the resonator, film and dielectric losses, and also the radiation loss, may influence the quality factor $Q$ of the CPW resonator. For the present device, i.e. niobium film deposited on the silicon substrate, the film and dielectric losses are very small at very low temperature ($T \ll T_c$, $T_c$ = 9.2 K for niobium). The radiation loss is also negligible, as the line width of the transmission line is very narrow. As a consequence, at $T \ll T_c$ the quality factor $Q_c$, related mainly to the coupling capacitance, dominates the loaded (total) quality factor $Q_l$ defined by

$$\frac{1}{Q_l} = \frac{1}{Q_i} + \frac{1}{Q_c}. \quad (3)$$

Here, $Q_i$ is the internal (unloaded) quality factor, accounting for the energy leakage due to all other losses. The coupling region of our device is designed as a coupling capacitor: a part of the CPW resonator is parallel and close to the through line. Although $Q_c$ cannot be calculated from coupling strength analytically, numerical simulations show that a weak coupling leads to a high quality factor. Therefore, the designed $Q_c$ can be adjusted by changing either the length of the CPW resonator parallel to the through line or the distance between them. Certainly, the coupling strength should not be set extremely small; otherwise the CPW resonator will not be excited for observation. The numerical results, considering our current fabrication techniques, show that, if the geometry parameters for the coupling region are set as those in Figure 1(c), then the desired quality factor could be up to 10$^6$.

After the above design and relevant numerical simulations, we fabricated our CPW resonator devices by magnetron

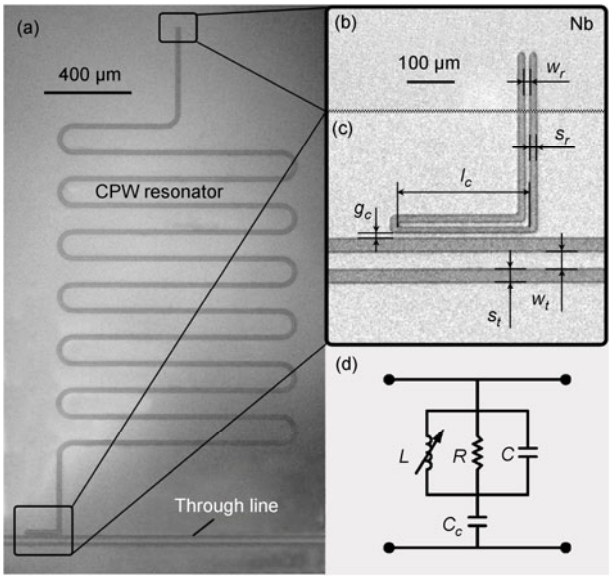


**Figure 1** (a) Microscope photograph of the key structure of our device. Light and dark areas are niobium film and silicon substrate, respectively. The through transmission line is used for excitation and readout. The meandered CPW resonator has an overall length of 15.814 mm, corresponding to a fundamental frequency around 1.8575 GHz. (b) One end of the CPW resonator is shorted to the ground plane. (c) The magnified coupling region and main design parameters: The length of the capacitor elbow $l_c$ is 160 μm and the distance between through line gap and the capacitor elbow gap $g_c$ is 7 μm. The width of center conductor $w_r$ and the gap between center conductor and ground $s_r$ are both 7 μm. (d) The equivalent circuit of the measured device.

sputtering and photolithography technique. Experimentally, a 160 nm thick niobium film was deposited on a 500 μm thick silicon substrate, and then contact exposure as well as reflect ion etching are used to make the desired patterns on the film.

The device can be treated equivalently as a measured parallel lumped RLC resonant circuit, shown in Figure 1(d), where $R$, $L$ and $C$ characterize the small resistance, inductance and capacitance of the measured CPW resonator, respectively. $C_c$ is the coupling capacitance between through line and the CPW resonator. Note that the total inductance of the CPW resonator: $L = L_m+L_k$, consists of two parts: the magnetic inductance $L_m$ and the kinetic inductance $L_k$ [19]. In particular, the latter one depends strongly on the temperature of the superconducting device. With such a property, the CPW resonator could be used as an attractive candidate of sensitive radiation detector.

The CPW resonator chip is glued (with GE varnish) onto a gold-plated sample block made of oxygen-free high purity copper and wire bonded to microwave transmission lines on a printed circuit board which was carefully designed to ensure a good performance up to 6 GHz microwave signals.

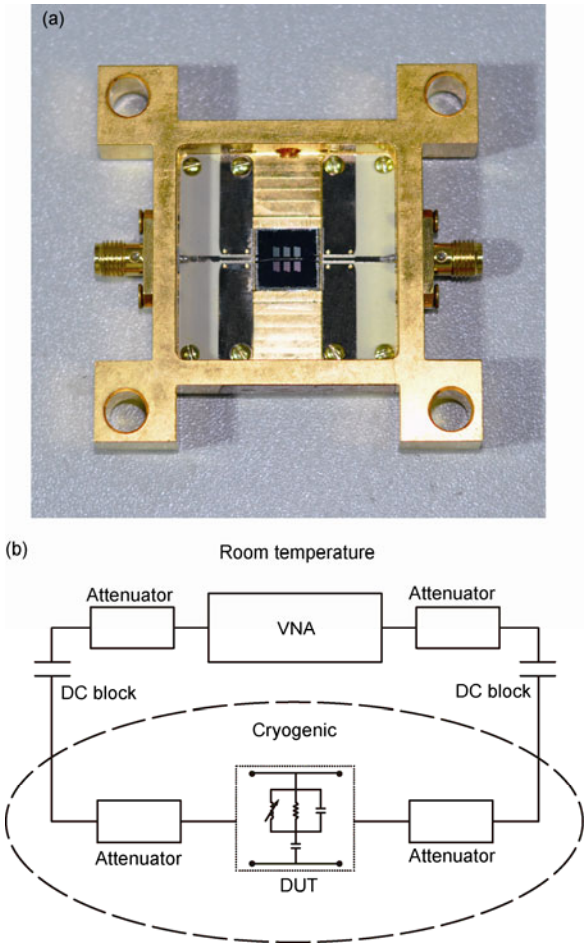


**Figure 2** Inner view of the sample block (a) and schematics of the measurement system (b).

Additional bonds are placed at all chip sides for good ground-connection. During the measurements the sample block is placed at the mixing chamber plate in our dilution refrigerator. Figure 2(b) shows the schematics of our measurement system. Cryogenic coax cables connect the sample block to room temperature circuits. Attenuators and DC blocks are positioned appropriately to reduce unwanted circuit noises. The device is measured with the Agilent E5071C vector network analyzer (VNA). The raw data collected consists of complex transmission amplitude $S_{21}$ for 1601 points in the desired frequency interval. Since the data is not calibrated, losses in the coax cables are included.

## 2 Experimental results

By sweeping the frequency and adjusting the power of VNA, the $S_{21}$ data were obtained and a resonance dip near the designed position was identified. It is observed that the shape of the resonance dip strongly depends on the driving power. For higher power, various nonlinear effects reveal and the resonance features of the device are complicated. While within the lower power regime, a maximum resonance dip depth was observed for an optimal driving power [21]. Indeed, it is seen from Figure 3 that, at the driving power –46 dBm an optimal resonance dip with a sufficiently high signal to noise ratio was found around 1.8575 GHz. Note that the present data include all the losses in the coax cables, which are estimated to be about −14 dB (at 1.8575 GHz). The inset of Figure 3 shows a sharper dip, corresponding to the same measurement with a wider bandwidth view.

From the obtained $S_{21}$ data, the loaded (total) quality factor of the CPW resonator can be calculated as

$$Q_l = \frac{f_0}{\Delta f}, \tag{4}$$

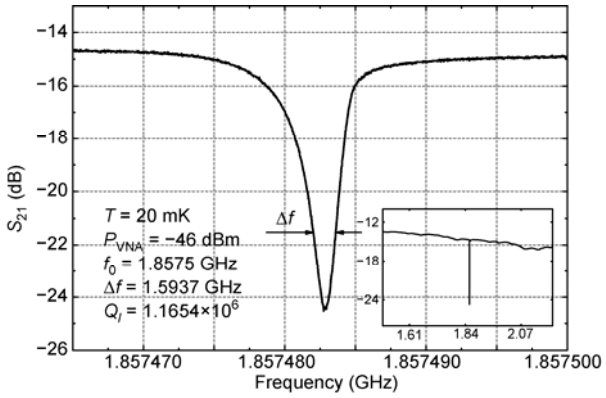


**Figure 3** The observed transmission dip. From the obtained $S_{21}$ data, one can calculate the loaded quality factor of the measured CPW resonator: $Q_l = f_0/\Delta f = 1.1654\times10^6$. The inset shows a sharper resonance dip, corresponding to the same measurements with a wider bandwidth view.

with $f_0$ being the resonance frequency and $\Delta f$ the 3 dB-bandwidth. $Q_l$ includes both the source and load dissipation of the device. In our case, $f_0$ =1.8575 GHz and $\Delta f$ = 1.5937 KHz were observed. Thus, the loaded quality factor is calculated as $Q_l = 1.1654\times10^6$. Also, $Q_i$ and $Q_c$ can be individually calculated from the minimal values of the measured $S_{21}$ parameters at the resonance point, i.e.$Q_i = Q_l/|S'_{21}|$. And $Q_c = Q_l\ (1-|S'_{21}|)$, with = min$\{S_{21}\}$. For our device, we found $Q_i = 3.2845\times10^6$ and $Q_c = 1.8063\times10^6$.

Furthermore, we measured the temperature dependence of the resonance frequency and quality factor by slowly enhancing the system temperature, e.g. from 30 to 1180 mK. We can see clearly from Figure 4 that, with increasing temperature, the center frequency shifts to higher value and the resonance dip becomes broader and shallower. Phenomenally, these behaviors can be explained in the framework of the two-level systems (TLSs) theory [22,23], in which the unsaturated TLSs residing on the metal and dielectric surfaces are believed to be a significant loss mechanism. The resonant interaction of TLSs with electric field (microwave) leads to a temperature dependent variation of the substrate dielectric constant. As a consequence, both dielectric constant $\epsilon$ and the surface inductance $L_s$ determine the resonance frequency as

$$\frac{\delta f}{f} = \frac{1}{2}\frac{\delta L_s}{L_s} - \frac{F}{2}\frac{\delta \epsilon}{\epsilon}, \tag{5}$$

where $F$ is a filling factor and $L_s = L_m + L_k(0)\times H(T)$. The magnetic inductance $L_m$ remains essentially a constant in the concerned temperature range. While, $H(T)$ represents the temperature dependence of the kinetic inductance $L_k$, which is strongly influenced by the temperature variation near the critical temperature $T_c$. However, at the present ultra-low temperature $T \ll T_c$ ($T_c$ = 9.2 K for niobium), the kinetic inductance can still be treated as a constant. Thus, the observed resonance frequency shifts were mainly related to the temperature-dependent dielectric constant. Indeed, it was shown that the dielectric constant decreases with temperature, and thus the resonance frequency of the CPW resonator increases. Certainly, if the device works at the temperature closing to $T_c$, then the effects due to TLSs saturate and the temperature dependence of kinetic inductance is dominant. Therefore, the increasing $L_k$ decreases the resonance frequency. Basically, the surface resistance $R_s$ increases with temperature monotonically, therefore the resonance dip is broader and shallower (and thus the quality factor decreases) for the increasing temperature.

## 3 Discussion and conclusions

The main advantage of superconducting CPW resonator device is that it can be easily integrated. That is, multiple resonators operating at different frequencies can be read out through a common feedline. In fact, the number of the multiplexed resonators depends on several factors, e.g. dvice quality factors and manufacture accuracy. In principle, a device with higher-$Q$ and better manufacture accuracy allows for a smaller frequency separation and thus more resonators multiplexed on one chip.

In order to make a simple presentation of frequency domain multiplexing scheme, we also fabricated a device with six resonators coupled to a common through line. Each resonator is designed with a different length, corresponding to a different resonance frequency. Figure 5 shows the measured results of such a multiplexed device, where six resonance dips can be observed expectably. One can see from the Table 1 that, the measured resonance frequency $f_m$ agrees well with the designed resonance frequency $f_t$. Specifically, the designed length of the resonator No. 5 is the same as that measured in Figure 3. The small difference (about 1.1 MHz) between the two measured resonance frequencies indicates that our devices are sufficiently accurate.

In summary, we have designed and fabricated a high-quality niobium quarter-wave CPW resonator. The transmission of microwave is measured with a vector network

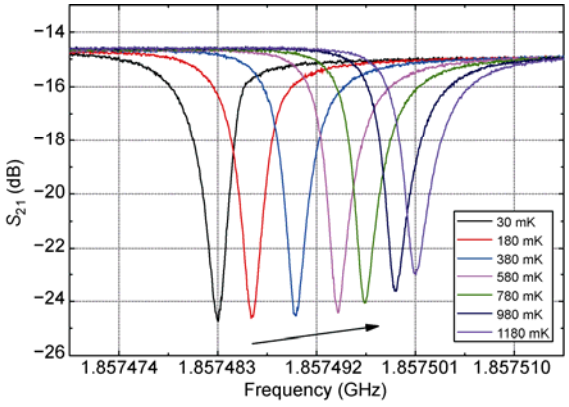


**Figure 4** The increasing resonance frequency and decreasing quality factor of the CPW resonator versus the increasing system temperature for $T \ll T_c$.

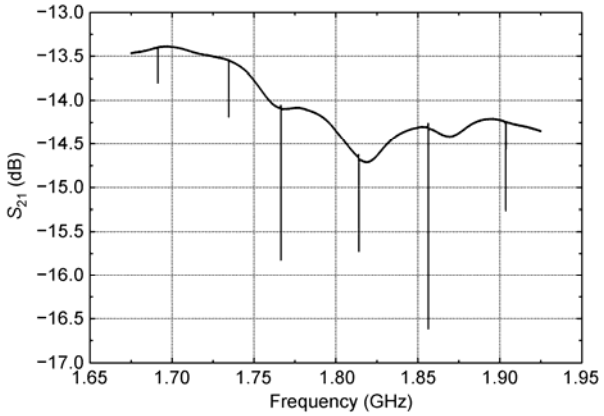


**Figure 5** Resonance dips for six resonators multiplexed on a chip.

**Table 1** Designed and measured resonance frequencies of six CPW resonators on a chip

| No. | $l_d$ (μm) | $f_t$ (GHz) | $f_m$ (GHz) |
|---|---|---|---|
| 1 | 17414 | 1.6958 | 1.6914 |
| 2 | 17014 | 1.7357 | 1.7346 |
| 3 | 16614 | 1.7775 | 1.7664 |
| 4 | 16214 | 1.8213 | 1.8139 |
| 5 | 15814 | 1.8674 | 1.8563 |
| 6 | 15414 | 1.9159 | 1.9037 |

analyzer and a sharp resonance dip is observed at designed position. At 20 mK, the measured quality factor of the device is $Q_l = 1.1654\times10^6$, which is significantly high and could be applied to sensitive radiation detections and quantum information processing.

*This work was supported by the National Natural Science Foundation of China (90921010, 11174373) and National Basic Research Program of China (2010CB923104).*

1 Day P K, LeDuc H G, Mazin B A, et al. A broadband superconducting detector suitable for use in large arrays. Nature, 2003, 425: 817–821
2 Mazin B A, Bumble B, Day P K, et al. Position sensitive X-ray spectrophotometer using microwave kinetic inductance detectors. Appl Phys Lett, 2006, 89: 222507
3 Day P K, Leduc H G, Goldin A, et al. Antenna-coupled Microwave kinetic inductance detectors. Phys Rev A, 2006, 559: 561–563
4 Tholén E A, Ergül A, Doherty E M, et al. Nonlinearities and parametric amplification in superconducting coplanar waveguide resonators. Appl Phys Lett, 2007, 90: 253509
5 Wallraff A, Schuster D I, Blais A, et al. Strong coupling of a single photon to a superconducting qubit using circuit quantum electrodynamics. Nature, 2004, 431: 162–167
6 Yu L B, Tong N H, Xue Z Y, et al. Simulation of the spin-boson model with superconducting phase qubit coupled to a transmission line. Sci China Phys Mech Astron, 2012, 55: 1557–1561
7 Amsüss R, Koller C, Nöbauer T, et al. Cavity QED with magnetically coupled collective spin states. Phys Rev Lett, 2011, 107: 060502
8 Zhou Z W, Chen W, Sun F W, et al. A survey on quantum information technology. Chin Sci Bull, 2012, 57: 1498–1525
9 Qian, Y, Zhang Y Q, Xu J B. Amplifying stationary quantum discord and entanglement between a superconducting qubit and a data bus by time-dependent electromagnetic field. Chin Sci Bull, 2012, 57: 1637–1642
10 Kubo Y, Diniz I, Grezes C, et al. Electron spin resonance detected by a superconducting qubit. Phys Rev B, 2012, 86: 064514
11 Irwin K, Hilton G, Wollman D, et al. X-ray detection using a superconducting transitionedge sensor microcalorimeter with electrothermal feedback. Appl Phys Lett, 1996, 69: 1945–1947
12 Chervenak J, Irwin K, Grossman E, et al. Superconducting multiplexer for arrays of transition edge sensors. Appl Phys Lett, 1999, 74: 4043–4045
13 Peacock A, Verhoeve P, Rando N, et al. Single optical photon detectionwith a superconducting tunnel junction. Nature, 1996, 381: 135–137
14 Shen D D, Zhu R, Xu W W, et al. Character and fabrication of Al/$Al_2O_3$/Al tunnel junctions for qubit application. Chin Sci Bull, 2012, 57: 409–412
15 You L X, Shen X F, Yang X Y, et al. Single photon response of superconducting nanowire single photon detector. Chin Sci Bull, 2010, 55: 441–445
16 Tinkham M, Emery V. Introduction to Superconductivity. 2nd ed. New York: Dover Publications, 1996
17 Jiang Y, Liang M, Jin B B, et al. A simple Fourier transform spectrometer for terahertz applications. Chin Sci Bull, 2012, 57: 573–578
18 Gao L, Guo J, Wang Y H, et al. A 23 GHz high-temperature superconducting microstrip filter for radio astronomy. Chin Sci Bull, 2009, 54: 3485–3488
19 Mazin B A. Microwave kinetic inductance detectors. PhD Thesis. California: California Institute of Technology Pasadena, 2004
20 Wadell B C. Transmission Line Design Handbook. Norwood, MA: Artech House Publishers, 1991
21 De Visser P J, Withington S, Goldie D J. Readout-power heating and hysteretic switching between thermal quasiparticle states in kinetic inductance detectors. J Appl Phys, 2010, 108: 114504
22 Gao J, Daal M, Martinis J M, et al. A semiempirical model for two-level system noise in superconducting microresonators. Appl Phys Lett, 2008, 21: 212504
23 Wisbey D S, Gao J, Vissers M R, et al. Effect of metal/substrate interfaces on radio-frequency loss in superconducting coplanar waveguides. J Appl Phys, 2010, 108: 093918